

## Splitting rules for the electronic energy spectra of two-dimensional Thue–Morse lattices with three kinds of atom and one bond length

This article has been downloaded from IOPscience. Please scroll down to see the full text article.

2005 J. Phys.: Condens. Matter 17 4747

(<http://iopscience.iop.org/0953-8984/17/30/003>)

View [the table of contents for this issue](#), or go to the [journal homepage](#) for more

Download details:

IP Address: 129.252.86.83

The article was downloaded on 28/05/2010 at 05:39

Please note that [terms and conditions apply](#).

# Splitting rules for the electronic energy spectra of two-dimensional Thue–Morse lattices with three kinds of atom and one bond length

Xubo Hu and Xiangbo Yang<sup>1</sup>

Institute of Laser Life Science, South China Normal University, Guangzhou 510631, People's Republic of China

E-mail: [xbyang@scnu.edu.cn](mailto:xbyang@scnu.edu.cn)

Received 11 May 2005, in final form 16 June 2005

Published 15 July 2005

Online at [stacks.iop.org/JPhysCM/17/4747](http://stacks.iop.org/JPhysCM/17/4747)

## Abstract

In this paper we study the splitting rules of the electronic energy spectra for two-dimensional Thue–Morse lattices with three kinds of atom and one bond length by means of a decomposition–decimation method. It is found that the symmetries of systems, boundary conditions, and then the branching types of energy spectra for the second and third hierarchies are all related to generations. For example, under the second-order approximation, the energy spectra of four-atom  $A$  molecules split in the proportion of one-to-five for even generations and one-to-three for odd ones. The analytical results are confirmed by numerical simulations.

## 1. Introduction

The pioneering experiments of Shechtman *et al* [1] have opened up an interesting field of solid-state physics—quasicrystal physics. Since then, much attention has been paid to the investigation of the electronic properties of quasilattices, especially the energy spectrum structure, which is an important aspect in the physical properties of quasicrystals. It is well known that for one-dimensional (1D) Fibonacci quasicrystals, the band structure, which is a Cantor-like set, shows a peculiar self-similarity because of its hierarchical geometric structure [2–4]. For two-dimensional (2D) Penrose tiling, its topological structure is much more complicated than its 1D counterparts; there is no unusual self-similarity to be found for its energy spectra [5–7] while the eigenstates do show self-similar features [8]. Another similar system is labyrinth tiling. Its energy spectra can be either band-like or fractal-like and the eigenstates are multifractal [9]. As regards a 2D Fibonacci quasilattice with one kind of atom and two kinds of length, Ueda and Tsunetsugu [10] investigated the energy spectrum and conductance numerically; its energy spectrum, density of states, and dynamical response function were studied analytically by Ashraff *et al* [11], and the results have been confirmed

<sup>1</sup> Author to whom any correspondence should be addressed.

by numerical simulations; Fu and Liu [12] investigated the rules of electronic energy spectra splitting by means of a decomposition–decimation (DD) method and found that its spectrum has a variety of multifurcating structures. Yang *et al* [13–16] investigated the splitting rules for the electronic spectra of 2D Fibonacci quasilattices (FC(1)) with three kinds of atom and one bond length, 2D Fibonacci-class quasilattices (FC( $n$ )) with one kind of atom and two bond lengths, and 2D SML quasilattices with one kind of atom and three bond lengths.

On the other hand, being a bridge of linking periodic systems with quasiperiodic ones in a geometrical structure, Thue–Morse (TM) systems have attracted considerable attention over the past years. Cheng *et al* [17] studied the structure and electronic properties of TM lattices and found that the structure factor is composed of a sequence of  $\delta$ -function peaks just like quasiperiodic systems. Based on a real space renormalization-group (RSRG) method, Ghosh and Karmakar [18] have studied the existence for extended eigenstates of the electronic and phonon problem for different models of the TM chain. Chattopadhyay and Chakrabarti [19] showed that a TM aperiodic structure presents a unique kind of positional correlation between its constituents, leading to an unattenuated transmission of light as well as electrons through it. Axel and Peyriere [20] studied the spectrum of a 1D harmonic chain with controlled disorder determined by the TM sequence and found that it is a Cantor-like set. Generalized TM (GTM) models have also been generated by some groups [21, 22]. Wang *et al* [23] studied the properties of trace and antitrace maps for GTM system.

In this paper, we study the splitting rules for the electronic energy spectra of 2D TM lattices with three kinds of atom and one bond length by means of a DD method. It is found that the branching types of energy spectra for the second and third hierarchies, symmetries of systems, and boundary conditions are all related to generations, and there exists one kind of new splitting proportion as one-to-two for some subbands and subsubbands. These properties are interesting and have not been found in quasilattices previously. In section 2, we introduce the construction method of this kind of TM lattice, and we study the splitting rules for spectra in section 3. In section 4, analyses of the influences on electronic energy spectra are given, and section 5 is a brief summary.

## 2. The 2D TM lattices with three kinds of atom and one bond length

With two building blocks denoted by  $A$  and  $B$ , a TM sequence can be constructed by the successive substitutions  $A \rightarrow AB$  and  $B \rightarrow BA$  [24]. Choosing  $A$  as the starting block, one can obtain the TM sequence as follows:

$$\begin{aligned} S_1 &= A, \\ S_2 &= AB = S_1 \overline{S_1}, \\ S_3 &= ABBA = S_2 \overline{S_2}, \\ &\dots\dots \\ S_{n+1} &= S_n \overline{S_n}, \end{aligned} \tag{1}$$

where the  $\overline{S_n}$  sequence is complementary to the  $S_n$  one [24].

The normal 2D TM aperiodic system has a network form constructed by 1D TM chains in the vertical and horizontal directions. The 2D TM lattices under study are different from the normal one and can be constructed in the following way. (1) Create two 1D TM chains in the same way along  $X$  and  $Y$  axes, respectively, where long denotes the  $A$  block and short denotes the  $B$  one. (2) By means of general multiplication we define long  $\times$  long =  $A$  atom, short  $\times$  short =  $B$  atom, and long  $\times$  short = short  $\times$  long =  $C$  atom. So the 2D TM lattices with three kinds of atom and one bond length, which are shown in figure 1, can be obtained.

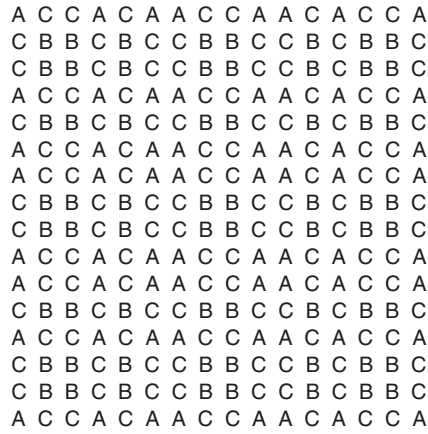


Figure 1. 2D Thue–Morse lattices with three kinds of atom and one bond length.

### 3. Splitting rules of spectra

#### 3.1. Numerical simulations of spectra

In the framework of the single-particle tight-binding model, atomic orbits are located at the centre of the cell. The Hamiltonian can be written as follows:

$$H = \sum_i |i\rangle E_i \langle i| + \sum_{i,j}' |i\rangle t_{ij} \langle j|, \tag{2}$$

where  $|i\rangle$  is the  $i$ th Wannier state,  $\sum_{i,j}'$  is the sum over the nearest-neighbour atoms, and  $t$  is the transfer-matrix element. Under the first-order approximation, we assume that the transfer-matrix element  $t_{ij}$  is the same ( $-1.0$ ) for all pairs of atoms that are nearest neighbour with each other and zero otherwise.  $E_i$  is the site energy, which can be different for different kinds of atom. Here we assume that  $E_A = -8.0$  for  $A$  atoms,  $E_B = 8.0$  for  $B$  atoms, and  $E_C = 0.0$  for  $C$  atoms, respectively, in order to separate the energy levels sufficiently to see the splitting and the influence of the interactions for different kinds of atom on the energy spectra. Figure 2 shows the numerical results of electronic energy spectra.

#### 3.2. Analytical results of spectra

In this part, we analyse the splitting manners for the electronic energy spectra by means of a DD method. The interaction between atoms with the same energy is the dominant factor to affect the spectra splitting of the subband; the interaction between the different kinds of atom or between atoms with different energy levels can be regarded as perturbations.

Under the zeroth-order approximation, we assume that there is no interaction among the atoms (i.e.,  $t_{ij} = 0$ ); then there are three kinds of isolated atom in the system and there exist only three highly degenerate energies  $E_A$ ,  $E_B$ , and  $E_C$ .

Furthermore, under the first-order approximation, we assume that there is an interaction only between the nearest-neighbour atoms; then there are nine kinds of isolated cluster in the system, which are shown in figure 3, i.e., the isolated  $A$  atoms, diatomic  $A$  molecules, four-atom  $A$  molecules, the isolated  $B$  atoms, diatomic  $B$  molecules, four-atom  $B$  molecules, the isolated  $C$  atoms, diatomic  $C$  molecules, and four-atom  $C$  molecules, and there exist fifteen energy levels:  $E_i \pm 2t$ ,  $E_i \pm t$  and  $E_i$  ( $i = A, B, C$ ). In fact, because of the symmetry of the energy spectra, the first and fifth subbands, the second and fourth ones, the sixth and tenth ones, the seventh and ninth ones, the eleventh and fifteenth ones, and the twelfth and the

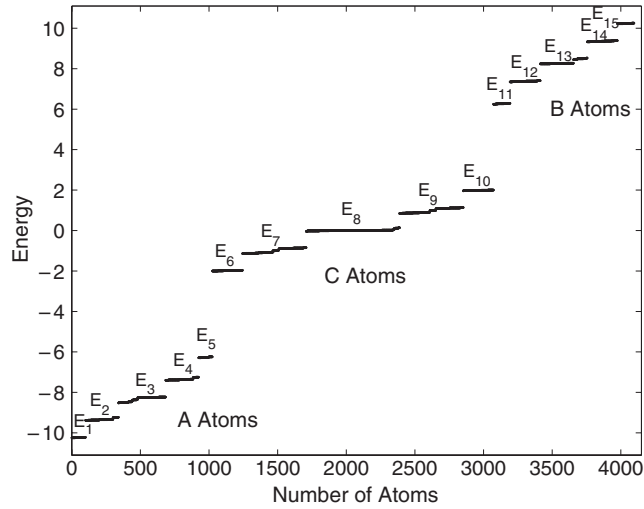


**Figure 2.** Electronic energy spectra of the 2D Thue-Morse lattices versus atom number with 4096 atoms, where  $E_A = -8.0$ ,  $E_B = 8.0$ ,  $E_C = 0.0$ , and  $t = -1.0$ . There are 15 subbands in the system.

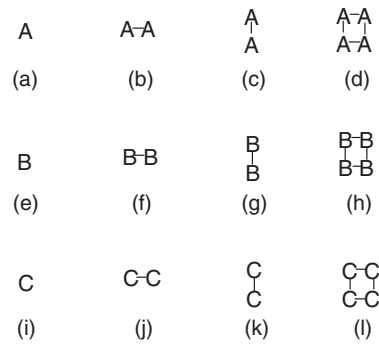


**Figure 3.** Nine kinds of cluster in the first renormalization procedure: (a) isolated A atom, (b) and (c) diatomic A molecules, (d) four-atom A molecule, (e) isolated B atom, (f) and (g) diatomic B molecules, (h) four-atom B molecule, (i) isolated C atom, (j) and (k) diatomic C molecules, (l) four-atom C molecule.

fourteenth ones, are identical. Therefore, only nine kinds of main subband exist. Based on the following analytical results we obtain the total spectral structure for the 2D TM lattices, which is schematically shown in figures 4 and 5.

**3.2.1. The first and fifth subbands ( $E_1$  and  $E_5$ ).** These subbands are formed by the energy levels  $E_{1,5} = E_A \pm 2t$  of four-atom A molecules. In performing the DD procedure for the four-atom molecule degenerate states, we have to investigate the coupling interactions in the following two cases:

(1) For even generations, there exist six types of coupling interaction shown as figure 6. For the strong interaction between atoms with the same state (i.e., diatomic C molecules, diatomic A molecules, etc), we choose matrix element  $t_s = -1.0$ . We choose  $t_w = -0.1$  for the weak interaction between atoms with different states. By means of the DD procedure the

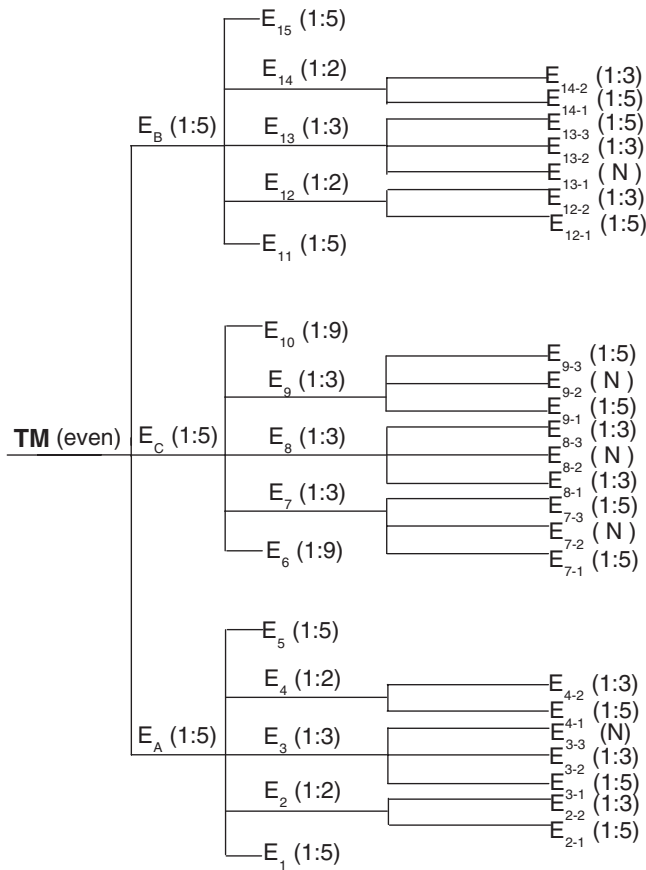


**Figure 4.** Total electronic energy spectral structure of 2D Thue–Morse lattices for even generations.

six kinds of corresponding renormalized transfer-matrix element can be obtained as follows:

$$T_a = 0, \quad T_b \approx T_c = -t_w^2/2t_s, \quad T_d \approx T_e \approx T_f = -t_w^2/t_s; \quad (3)$$

then we have

$$\begin{aligned} E_{1-1} &= E_A + 2t - T_d \\ E_{1-2} &= E_A + 2t - T_b \\ E_{1-3} &= E_A + 2t \\ E_{1-4} &= E_A + 2t + T_b \\ E_{1-5} &= E_A + 2t + T_d, \end{aligned} \quad (4)$$

and

$$\begin{aligned} E_{5-1} &= E_A - 2t - T_d \\ E_{5-2} &= E_A - 2t - T_b \\ E_{5-3} &= E_A - 2t \\ E_{5-4} &= E_A - 2t + T_b \\ E_{5-5} &= E_A - 2t + T_d. \end{aligned} \quad (5)$$

Therefore, the main subbands  $E_1$  and  $E_5$  of even generations split as one-to-five (see figure 4). As an example, figure 7 shows the enlarged first main subband  $E_1$  of the sixth generation.

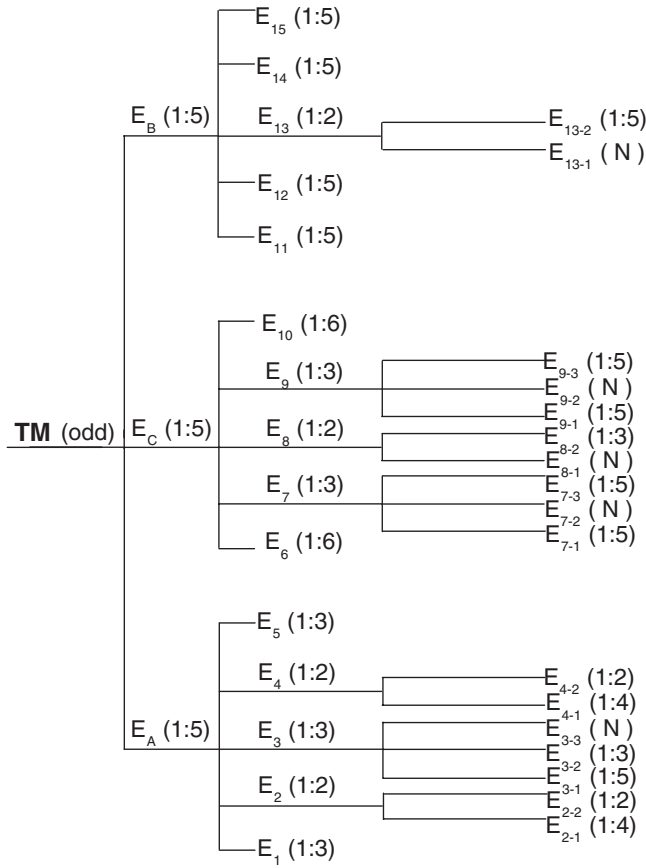


**Figure 5.** Total electronic energy spectral structure of 2D Thue–Morse lattices for odd generations.

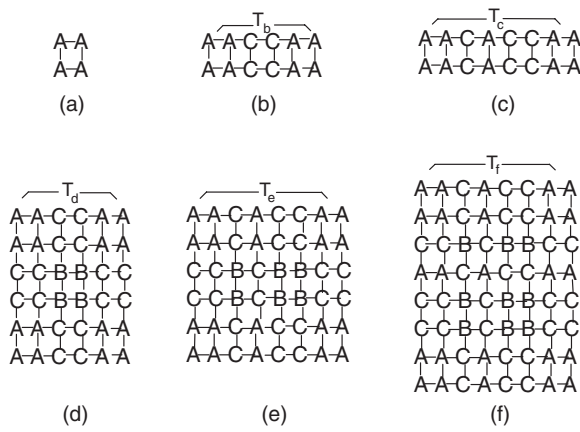


**Figure 6.** Six types of coupling interaction between four-atom A molecules.

(2) For odd generations, there are only four types of coupling interaction (see figures 6(a), (d)–(f)), and the subbands  $E_1$  and  $E_5$  all split as one-to-three (see figure 5). As an example, figure 8 shows the enlarged first main subband  $E_1$  of the seventh generation.

Obviously, for this kind of 2D TM lattice the splitting manners change with generations. The main reason is that the symmetry, boundary conditions, and the types of clusters, all

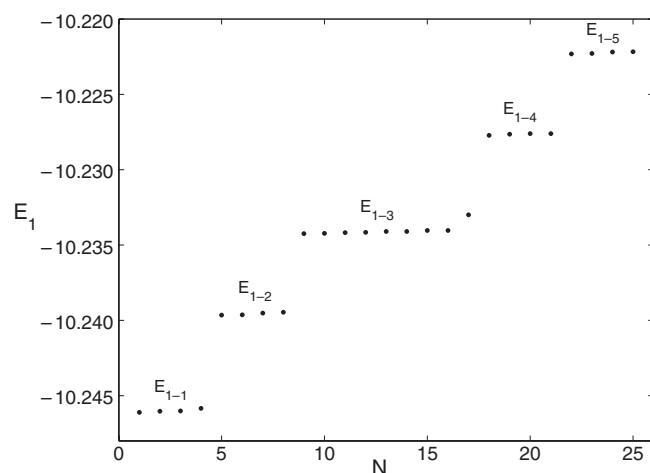


**Figure 7.** The enlarged first main subband  $E_1$  of the sixth generation, which has a five-subsubband structure.

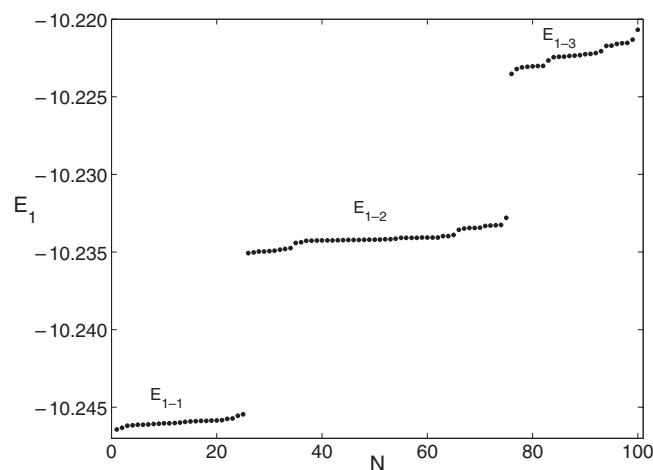


**Figure 8.** The enlarged first main subband  $E_1$  of the seventh generation, which has a three-subsubband structure.

change with generations. The systems of even generations are symmetric, while those of odd generations are asymmetric, and influences of boundary conditions in these systems are dominant for some subbands or subsubbands.

**3.2.2. The eleventh and fifteenth subbands ( $E_{11}$  and  $E_{15}$ ).** These subbands are formed by the energy levels  $E_{11,15} = E_B \pm 2t$  of four-atom  $B$  molecules. The coupling interactions, the corresponding renormalized transfer-matrix elements, and then the splitting manners, are all similar to those of four-atom  $A$  molecules of even generations (see figure 4). The main reason is that the structure of the sublattices of four-atom  $B$  molecules does not change with generations, and is the same as that of four-atom  $A$  molecules of even generations.

**3.2.3. The second and fourth subbands ( $E_2$  and  $E_4$ ).** These subbands are formed by the energy levels  $E_{2,4} = E_A \pm t$  of diatomic  $A$  molecules, and there exist six types of cluster, which are shown in figure 9; the main subband  $E_2$  will split as one-to-two (see figures 4, 5, 10, and 11). The case of  $E_4$  is the same as that of  $E_2$ .



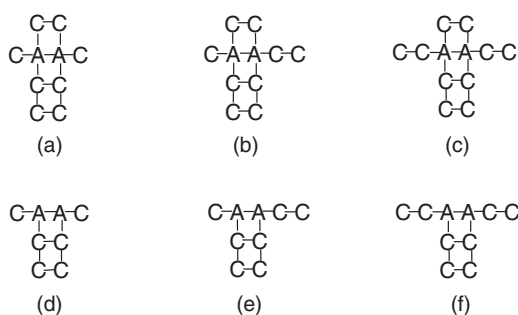


**Figure 9.** Six kinds of diatomic  $A$  molecule cluster, where the diatomic  $A$  molecules in (a)–(c) are inside systems and those in (d)–(f) are on boundaries.

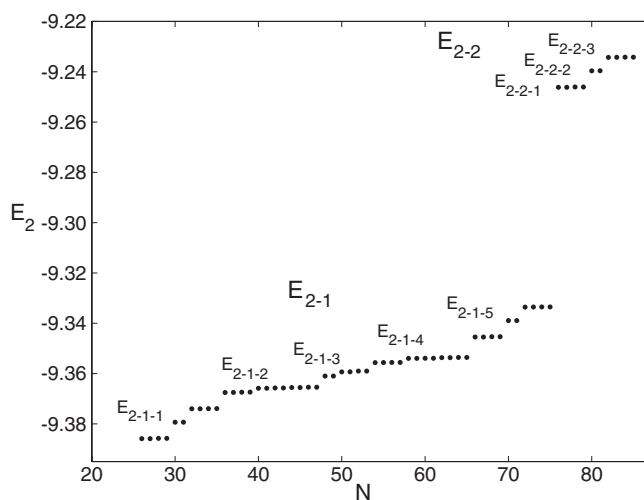


**Figure 10.** The enlarged second main subband  $E_2$  of the sixth generation, which has a two-subsubband structure. The 1:5 (one-to-five) splitting behaviour for the bottom subsubband and the 1:3 (one-to-three) splitting behaviour for the upper subsubband are clearly seen.

Furthermore, for the third hierarchy, (1) the subsubband  $E_{2-1}$  is formed by the three types of diatomic  $A$  molecule shown in figures 9(a)–(c), which are inside systems and construct ten kinds of coupling interaction shown as figure 12. By means of a DD method, one can obtain that the subsubband  $E_{2-1}$  will split as one-to-five (see figures 4 and 10). On the other hand, for odd generations, systems are asymmetric and there exist remarkable hybridized orbit phenomena. The subsubband  $E_{2-1}$  will split as one-to-four (see figures 5 and 11). (2) The subsubband  $E_{2-2}$  is formed by the three types of diatomic  $A$  molecule shown in figures 9(d)–(f), which are on boundaries and construct three types of coupling interaction shown as figure 13, and it will split as one-to-three (see figures 4 and 10); but for odd generations, the isolated diatomic  $A$  molecule shown as figure 13(a) does not exist on boundaries, and the subsubband  $E_{2-2}$  splits as one-to-two (see figures 5 and 11).

**3.2.4. The twelfth and fourteenth subbands ( $E_{12}$  and  $E_{14}$ ).** These subbands are formed by the energy levels  $E_{12,14} = E_B \pm t$  of diatomic  $B$  molecules; one can investigate the splitting problem in the following two cases.

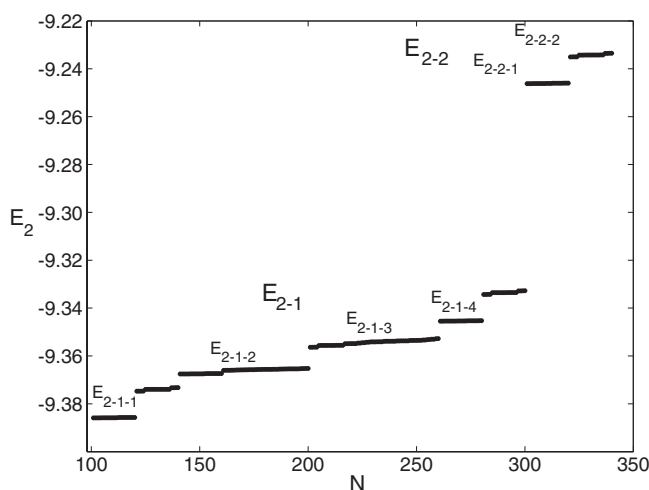


**Figure 11.** The enlarged second main subband  $E_2$  of the seventh generation, which has a two-subsubband structure. The 1:4 (one-to-four) splitting behaviour for the bottom subsubband and the 1:2 (one-to-two) splitting behaviour for the upper subsubband are clearly seen.

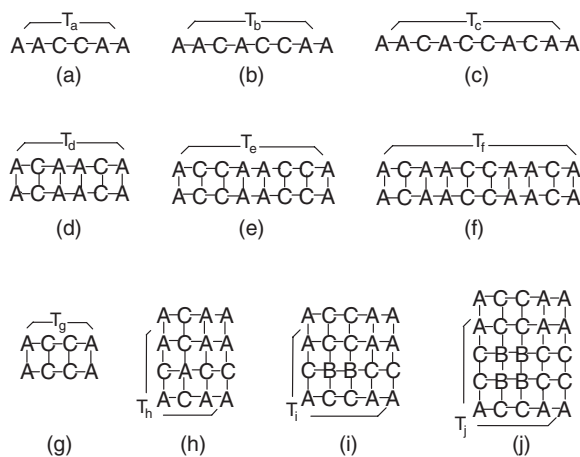


**Figure 12.** Ten types of coupling interaction systems between diatomic  $A$  molecules inside systems.

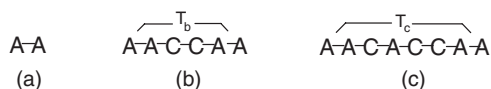


**Figure 13.** Three types of coupling interaction between diatomic  $A$  molecules on boundaries.

- (1) For even generations, the spectral structures of  $E_{12}$  and  $E_{14}$  are all the same as those of  $E_2$  (see figure 4) because of the symmetry of  $A$  and  $B$  atoms.
- (2) For odd generations,  $B$  atoms are all inside systems and there is no  $B$  atom on boundaries. The coupling interactions of diatomic  $B$  molecules are now the same as those of diatomic  $A$  molecules inside systems, which are shown as figure 12. Therefore, for odd generations the twelfth and fourteenth main subbands split as one-to-five (see figures 5 and 14).

**3.2.5. The third subband ( $E_3$ ).** This subband is formed by the threefold degenerate energy level  $E_3 = E_A$  of isolated  $A$  atoms and four-atom  $A$  molecules, and there are nine types of cluster shown as figure 15. By a DD method one can also obtain that the main subband  $E_3$  splits as one-to-three (see figures 4, 5, and 16).

For the third hierarchy, (1) the subsubband  $E_{3-1}$  is formed by the isolated  $A$  atoms shown in figure 15(c), which construct five types of coupling interaction shown as figure 17. By means

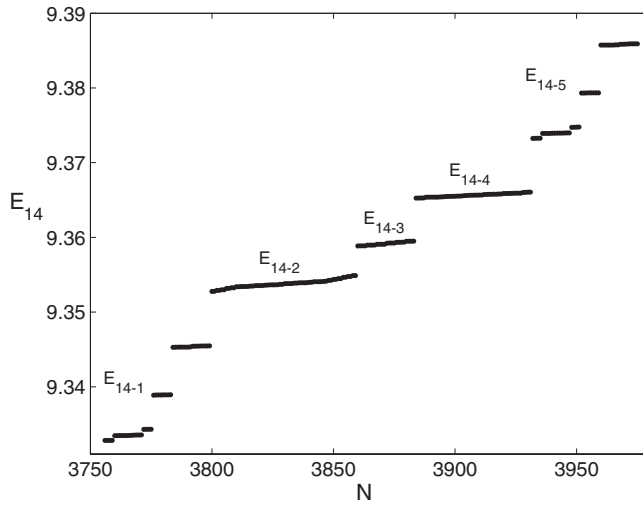


**Figure 14.** The enlarged fourteenth main subband  $E_{14}$  of the seventh generation, which has a five-subsubband structure.

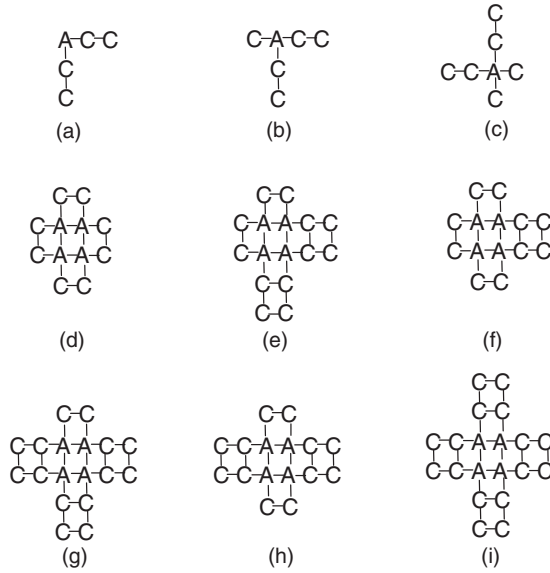


**Figure 15.** Nine kinds of isolated  $A$  atom and four-atom  $A$  molecule cluster, where the isolated  $A$  atom in (a) is at vertex, that in (b) is on edge, the isolated  $A$  atom in (c) and four-atom  $A$  molecules in (d)–(i) are all inside systems.

of a DD method, one can obtain the corresponding renormalized transfer-matrix elements as follows:

$$T_a = -t_w^2/t_s, \quad T_b = T_c = T_d = 0, \quad T_e = -2t_w^2/t_s; \quad (6)$$

then we have

$$\begin{aligned} E_{3-1-1} &= E_{3-1} - T_e \\ E_{3-1-2} &= E_{3-1} - T_a \\ E_{3-1-3} &= E_{3-1} \\ E_{3-1-4} &= E_{3-1} + T_a \\ E_{3-1-5} &= E_{3-1} + T_e. \end{aligned} \quad (7)$$

Therefore, the subsubband  $E_{3-1}$  splits as one-to-five (see figures 4, 5, and 16). (2) The subsubband  $E_{3-2}$  is formed by the isolated  $A$  atoms shown in figure 15(b), which construct

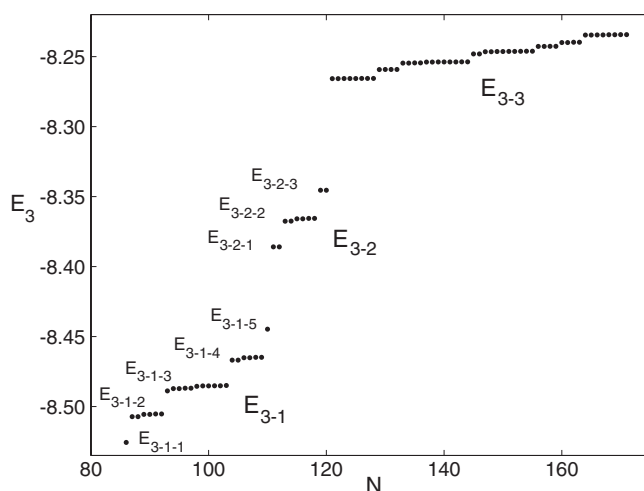


**Figure 16.** The enlarged third main subband  $E_3$  of the sixth generation, which has a three-subsubband structure. The 1:5 (one-to-five) splitting behaviour for the bottom subsubband and the 1:3 (one-to-three) splitting behaviour for the middle subsubband are clearly seen.

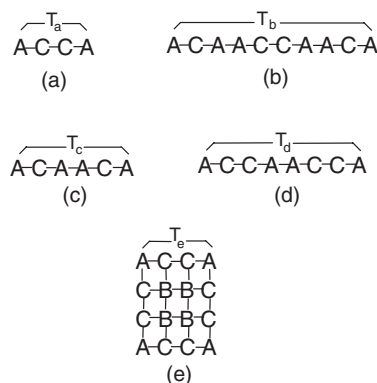


**Figure 17.** Five types of coupling interaction between the isolated  $A$  atoms.

four types of coupling interaction shown as figures 17(a)–(d). Using equation (6) one can deduce that the subsubband  $E_{3-2}$  splits as one-to-three (see figures 4, 5, and 16). (3) The subsubband  $E_{3-3}$  is formed by the isolated  $A$  atoms shown in figure 15(a) and the four-atom  $A$  molecules shown in figures 15(d)–(i), whose coupling interactions are very complex. Up to now the splitting manner of this subsubband has not been obtained.

**3.2.6. The thirteenth subband ( $E_{13}$ ).** This subband is formed by the threefold degenerate energy level  $E_{13} = E_B$  of the isolated  $B$  atoms and four-atom  $B$  molecules.

- (1) For even generations, the cases of  $E_{13}$  are similar to those of  $E_3$  because of the symmetry of  $A$  and  $B$  atoms, and it will split as one-to-three.
- (2) For odd generations, there is no  $B$  atom on boundaries and isolated  $B$  atom clusters similar to those shown in figures 15(a) and (b) do not exist; therefore, the main subband  $E_{13}$  for odd generations splits as one-to-two, the subsubband  $E_{13-2}$  is similar to that of

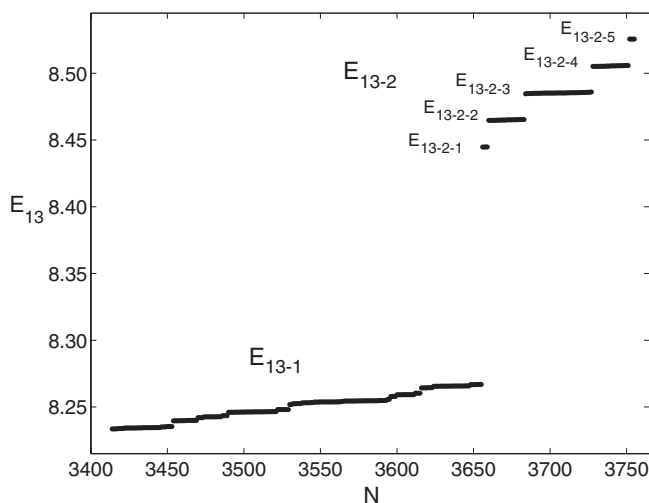


**Figure 18.** The enlarged thirteenth main subband  $E_{13}$  of the seventh generation, which has a two-subsubband structure. The 1:5 (one-to-five) splitting behaviour for the upper subsubband is clearly seen.

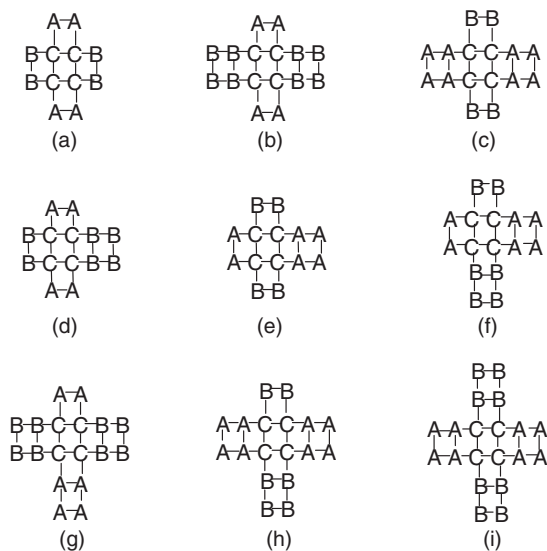


**Figure 19.** Nine kinds of four-atom  $C$  molecule cluster.

the subsubband  $E_{3-1}$  and splits as one-to-five, the subsubband  $E_{13-1}$  will be similar to that of the subsubband  $E_{3-3}$  and its splitting type is still unknown (see figures 5 and 18).

**3.2.7. The sixth and tenth subbands ( $E_6$  and  $E_{10}$ ).** These two subbands are formed by the levels  $E_{6,10} = E_C \pm 2t$  of four-atom  $C$  molecules. There are nine kinds of cluster, which are shown in figure 19.

- (1) For even generations, by means of the aforementioned method one can obtain that the two main subbands  $E_6$  and  $E_{10}$  split in the way of one-to-nine for even generations. As an example, figure 20 shows the enlarged tenth main subband  $E_{10}$  of the sixth generation.
- (2) On the other hand, from figure 19 one can see that all of the four-atom  $C$  molecules only interact with diatomic  $A$ , four-atom  $A$ , diatomic  $B$ , and four-atom  $B$  molecules. But for odd generations the proportion of diatomic  $B$  molecules with strong polarity is smaller

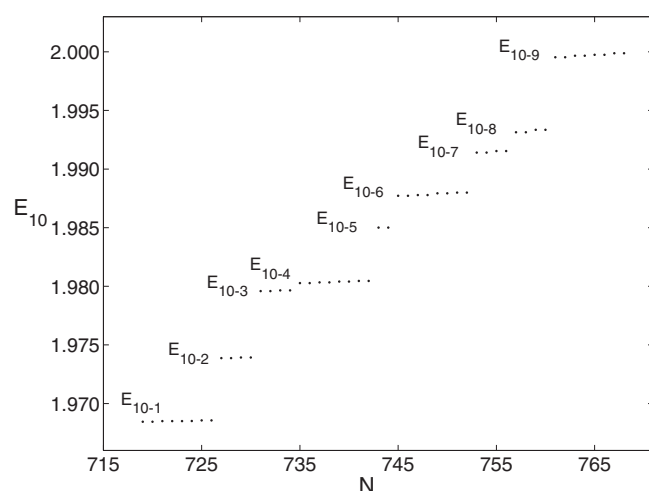


**Figure 20.** The enlarged tenth main subband  $E_{10}$  of the sixth generation, which has a nine-subsubband structure.

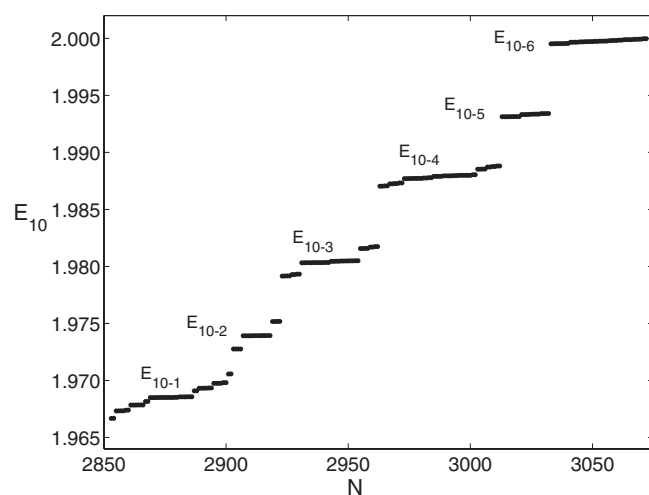


**Figure 21.** The enlarged tenth main subband  $E_{10}$  of the seventh generation, which has a six-subsubband structure.

than that of even generations. This modification will cause changes of the shape, the position, and the splitting manner of the two main subbands; then  $E_6$  and  $E_{10}$  will split in the way of one-to-six for odd generations. Figure 21 shows the splitting result of  $E_{10}$  of the seventh generation.

**3.2.8. The seventh and ninth subbands ( $E_7$  and  $E_9$ ).** These subbands are formed by the energy levels  $E_{7,9} = E_C \pm t$  of diatomic  $C$  molecules.

- (1) For even generations, there exist twelve types of corresponding cluster, which are shown in figure 22. For the clusters shown in figures 22(a)–(c) the dominant interaction comes from the repelling of diatomic  $A$  polar molecules, while for those in figures 22(d)–(f) the diatomic  $A$  polar molecules are replaced by the diatomic  $B$  ones, but the eigenenergy of the former is lower than that of the later. Therefore the three types of cluster in figures 22(a)–(c) form the subsubband  $E_{7-3}$ , while those in figures 22(d)–(f) form the subsubband  $E_{7-1}$ . For the clusters on boundaries shown in figures 22(g)–(l), the dominant effect is the interaction



**Figure 22.** Twelve kinds of diatomic  $C$  molecule cluster, where the diatomic  $C$  molecules in (a)–(f) are inside systems and those in (g)–(l) are on boundaries.

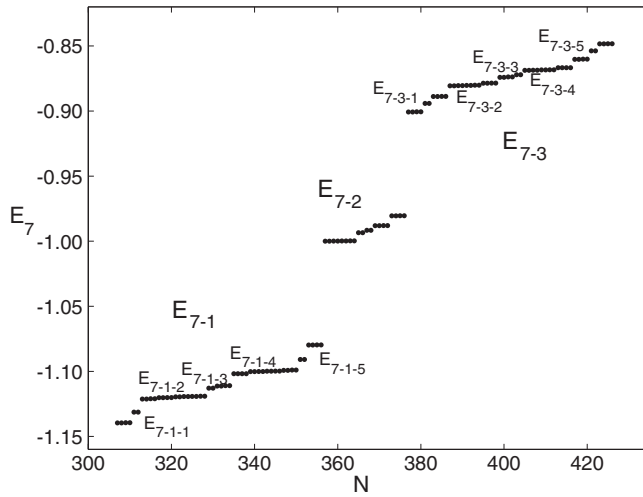


**Figure 23.** The enlarged seventh main subband  $E_7$  of the sixth generation, which has a three-subsubband structure. The 1:5 (one-to-five) splitting behaviour for the bottom subsubband and the 1:5 (one-to-five) splitting behaviour for the upper subsubband are clearly seen.

between diatomic  $C$  molecules and nonpolar four-atom  $A$  or  $B$  molecules, so the original energy level changes very slightly and it forms subsubband  $E_{7-2}$ . In conclusion, the main subbands  $E_7$  and  $E_9$  split as one-to-three (see figure 4). As an example, figure 23 shows the enlarged main subband  $E_7$  of the sixth generation.

- (2) For odd generations,  $B$  atoms do not occur on boundaries and there are only nine types of diatomic  $C$  molecule cluster (see figures 22(a)–(i)), but the main subbands  $E_7$  and  $E_9$  still split as one-to-three (see figure 5). The main reason is that the clusters shown in figures 22(j)–(l) are all on boundaries and possess the same kind of characteristics of those shown in figures 22(g)–(i).

Furthermore, for the third hierarchy, the subsubband  $E_{7-1}$  is formed by the diatomic  $C$  molecules shown in figures 22(d)–(f), which construct eight kinds of coupling interaction shown as figure 24. By means of a DD method, one can obtain the corresponding renormalized transfer-matrix elements as follows:

$$T_a \approx T_b = -t_w^2/2t_s, \quad T_d = -t_w^2/t_s, \quad T_i = 0 \quad (i = c, e, f, g, h); \quad (8)$$

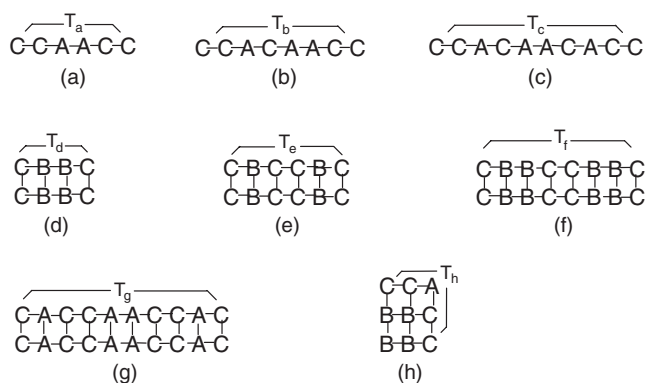


**Figure 24.** Eight types of coupling interaction between diatomic  $C$  molecules for the clusters shown in figures 22(d)–(f).

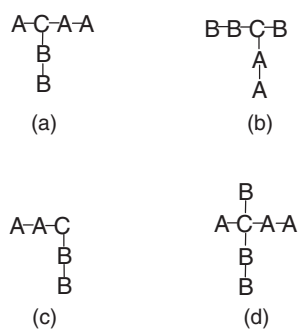


**Figure 25.** Four kinds of isolated  $C$  atom cluster, where the isolated  $C$  atoms in (a) and (b) are on boundaries, that in (c) is at a vertex, and that in (d) is inside a system.

then we have

$$\begin{aligned}
 E_{7-1-1} &= E_{7-1} - T_d \\
 E_{7-1-2} &= E_{7-1} - T_a \\
 E_{7-1-3} &= E_{7-1} \\
 E_{7-1-4} &= E_{7-1} + T_a \\
 E_{7-1-5} &= E_{7-1} + T_d.
 \end{aligned} \tag{9}$$

Therefore, the spectra split as one-to-five (see figures 4, 5, and 23). The subsubband  $E_{7-3}$  will split in the same way as that of  $E_{7-1}$  because of the symmetry (see figures 4, 5, and 23).

**3.2.9. The eighth subband ( $E_8$ ).** This subband is formed by the degenerate energy level  $E_8 = E_C$  of isolated  $C$  atoms and four-atom  $C$  molecules.

(1) For even generations, there exist four types of isolated  $C$  atom cluster (see figure 25) and nine types of four-atom  $C$  molecule cluster (see figure 19). For the isolated  $C$  atom cluster shown in figure 25(a) the dominant interaction comes from the repelling of diatomic  $A$  polar molecule on the edge, while for that in figure 25(b) the diatomic  $A$  polar molecule is replaced by the diatomic  $B$  one, but the eigenenergy of the former is lower than that of the latter, so the cluster in figure 25(a) forms the subsubband  $E_{8-3}$  while that in figure 25(b) forms the subsubband  $E_{8-1}$ . For the cluster shown in figure 25(c) the interaction between isolated  $C$  atom and diatomic  $A$  molecule is approximately equal to that between isolated  $C$  atom and diatomic  $B$  molecule; for the cluster shown in figure 25(d) and the ones shown in figure 19 the isolated  $C$  atom and four-atom  $C$  molecules do not interact with  $A$  or  $B$  atoms on boundaries. Their energy levels will all change slightly, and they form subsubband  $E_{8-2}$ . In a word, the



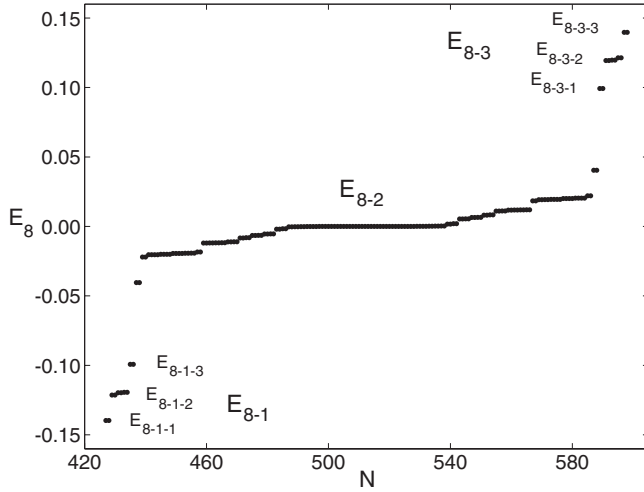


**Figure 26.** The enlarged eighth main subband  $E_8$  of the sixth generation, which has a three-subsubband structure. The 1:3 (one-to-three) splitting behaviours for the bottom and the upper subsubbands are clearly seen.

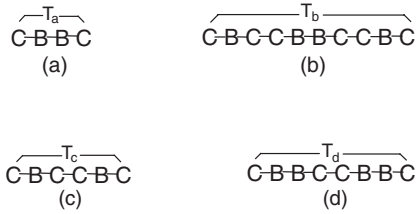


**Figure 27.** Four types of coupling interaction between the isolated  $C$  atoms for the cluster shown in figure 25(b).

main subband  $E_8$  splits as one-to-three (see figure 4). As an example, figure 26 shows the enlarged main subband  $E_8$  of the sixth generation. For the third hierarchy, the subsubband  $E_{8-1}$  is formed by the isolated  $C$  atoms shown in figure 25(b), which construct four kinds of coupling interaction shown as figure 27. By means of a DD method, one can obtain the corresponding renormalized transfer-matrix elements as follows:

$$T_a = -t_w^2/t_s, \quad T_i = 0 \quad (i = b \sim d); \quad (10)$$

then we have

$$\begin{aligned} E_{8-1-1} &= E_{8-1} - T_a \\ E_{8-1-2} &= E_{8-1} \\ E_{8-1-3} &= E_{8-1} + T_a. \end{aligned} \quad (11)$$

Therefore, the subsubband  $E_{8-1}$  splits as one-to-three (see figures 4 and 26). Similarly, the subsubband  $E_{8-3}$  will split in the same way as that of  $E_{8-1}$  because of the symmetry (see figures 4 and 26).

(2) For odd generations, the clusters shown in figures 25(b) and (c) do not exist. On the basis of the aforementioned analysis one can deduce that the main subband  $E_8$  splits as one-to-two (see figure 5). As an example, figure 28 shows the enlarged main subband  $E_8$  of the seventh generation.

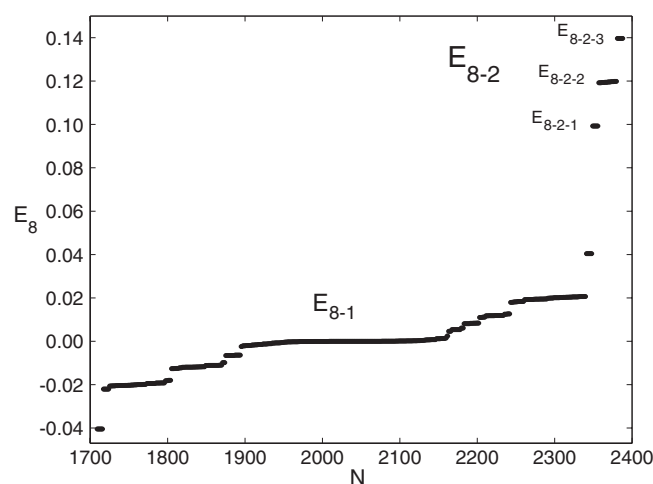


**Figure 28.** The enlarged eighth main subband  $E_8$  of the seventh generation, which has a two-subsubband structure. The 1:3 (one-to-three) splitting behaviour for the upper subsubband is clearly seen.

#### 4. Influence on the energy spectra

##### 4.1. Change of the splitting manners of energy spectra

In this paper we study the splitting rules of the electronic energy spectra for 2D TM lattices with three kinds of atom and one bond length by means of a DD method. It is found that the splitting types for higher hierarchies are all related to generations; for example, for the second hierarchy, the splitting manners of the main subbands  $E_i$  ( $i = 1, 5, 6, 8, 10, 12, 13, 14$ ) for even generations are different from those for odd generations; and for the third hierarchy, the splitting types of the subsubbands  $E_{i-j}$  ( $i = 2, 4; j = 1, 2$ ) for even generations are different from those for odd generations. The main reason is that systems for even generations are symmetric about  $A$  and  $B$  atoms, but for odd generations the symmetry will be destroyed. On the other hand, the boundary conditions for even generations are also different from those for odd generations, for there does not exist any  $B$  atom on boundaries for odd generations.

##### 4.2. Change of the position of energy spectra

The ‘bare energies’ of  $A$ ,  $B$ , and  $C$  atoms are  $E_A = -8.0$ ,  $E_B = 8.0$ , and  $E_C = 0.0$ , respectively, but numerical calculations show that the centres of the corresponding subbands of  $A$ ,  $B$ , and  $C$  atoms are located at  $-8.27$ ,  $8.30$ ,  $0.0$ , respectively, i.e., the centre of the energy spectra of  $A$  atoms shifts downwards and that of  $B$  atoms shifts upwards because of the interactions with  $C$  atoms. The number of diatomic  $C$  molecules with strong polarity is nearly twice as much as that of diatomic  $A$  (or  $B$ ) molecules.

##### 4.3. Change of the shape of energy spectra

The interactions between different kinds of atom and the boundary conditions change not only the position of energy subbands, but also the shape of energy spectra structure, which is symmetrical to the energy level  $0.0$  for even generations but asymmetrical for odd generations; for example, the shape of the main subband  $E_6$  is quite different from that of  $E_{10}$ . This phenomenon is like the formation of a hybridized orbit, and the practical energy spectral picture is some different from the standard one.

## 5. Brief summary

In this paper, the construction method of the 2D TM lattices with three kinds of atom and one bond length is presented and the splitting rules for the energy spectra are analysed by means of a DD method. Under the first-order approximation, there are nine kinds of isolated cluster and the electronic energy spectra split in the way of one-to-fifteen. Under the second-order approximation, the splitting manners of main subbands of  $E_i$  ( $i = 1, 5, 6, 8, 10, 12, 13, 14$ ) for even generations will be different from those for odd generations. Similar phenomena will also occur in higher hierarchies of energy spectra. The main reason is that symmetries of systems and the boundary conditions are all related to generations. On the other hand, interactions between different kinds of atom change not only the position of energy subbands, but also the shape of energy spectra structure. The analytic results are confirmed by numerical simulations.

## Acknowledgment

This work was supported by the National Nature Science Foundation of China, Grant No 10004003.

## References

- [1] Shechtman D, Blech I, Gratias D and Cahn J W 1984 *Phys. Rev. Lett.* **53** 1951
- [2] Zheng W M 1987 *Phys. Rev. A* **35** 1467
- [3] Liu Y and Riklund R 1987 *Phys. Rev. B* **35** 6034
- [4] Nori F and Rodriguez J P 1986 *Phys. Rev. B* **34** 2207
- [5] Ma P and Liu Y 1989 *Phys. Rev. B* **39** 9904
- [6] Kohmoto M and Sutherland B 1986 *Phys. Rev. B* **34** 3849  
Kohmoto M and Sutherland B 1986 *Phys. Rev. Lett.* **56** 2740
- [7] Odagaki T and Nguyen D 1986 *Phys. Rev. B* **33** 2184
- [8] Repetowicz P, Grimm U and Schreiber M 1998 *Phys. Rev. B* **58** 13482
- [9] Yuan H Q, Grimm U, Repetowicz P and Schreiber M 2000 *Phys. Rev. B* **62** 15569
- [10] Ueda K and Tsunetsugu H 1987 *Phys. Rev. Lett.* **58** 1272
- [11] Ashraff J A, Luck J-M and Stinchcombe R B 1990 *Phys. Rev. B* **41** 4314
- [12] Fu X, Liu Y, Chen B and Zheng D 1991 *Phys. Rev. B* **43** 10808
- [13] Yang X and Liu Y 1997 *Phys. Rev. B* **56** 8054
- [14] Yang X and Xing D 2002 *Phys. Rev. B* **65** 134205
- [15] Li F and Yang X 2004 *Eur. Phys. J. B* **39** 475
- [16] Chen F, Yang X, Xing D and Li F 2004 *Physica B* **353** 336
- [17] Cheng Z, Savit R and Merlin R 1988 *Phys. Rev. B* **37** 4375
- [18] Ghosh A and Karmakar S N 1998 *Phys. Rev. B* **58** 2586  
Ghosh A and Karmakar S N 2000 *Phys. Rev. B* **61** 1051
- [19] Chattopadhyay S and Chakrabarti A 2000 *J. Phys.: Condens. Matter* **12** 5681
- [20] Axel F and Peyriere J 1989 *J. Stat. Phys.* **57** 1013
- [21] Kolář M, Ali M K and Nori F 1991 *Phys. Rev. B* **43** 1034
- [22] Tao R 1994 *J. Phys. A: Math. Gen.* **27** 5069
- [23] Wang X, Grimm U and Schreiber M 2000 *Phys. Rev. B* **62** 14020
- [24] Thue A 1906 *Norske Vididensk. Selsk. Skr. I.* **7** 1  
Morse M 1921 *Trans. Am. Math. Soc.* **22** 84